

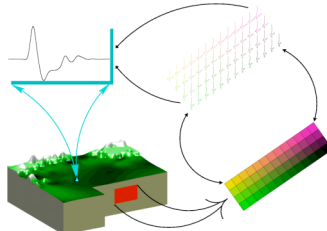


1 Introduction

There are theoretical considerations suggesting that observations and/or calculations of the rotational part of earthquake-induced ground motions may provide additional information on source and/or structure.

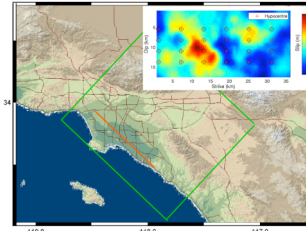
We carry out a systematic study of earthquake scenario simulations in 3-D media with a specific focus on the rotational part of the motions. We simulate several M7 earthquakes with various hypocenter location but identical slip distribution on the Newport-Inglewood (NI) fault embedded in the 3-D Los Angeles Basin. We use a recently calculated data base with several hundred numerical Green's functions for a discretized model of the NI fault allowing arbitrary finite-fault scenarios to be synthesized by superposition. We investigate source and basin structure effects on the rotational components of ground motion (e.g., peak ground rotation rates and their variation, horizontal gradients) and compare with the effects on translations.

2 Numerical Green's Function Method



We calculate numerical "Green's" functions (NGFs) for strike slip excitation on a discretized version of a specific fault embedded in a 3-D medium. The NGFs – calculated for a specific subfault size – are then synthesized for arbitrary slip histories (within some limits). This allows systematic investigation of source-related variations of ground motion parameters for a specific 3-D area.

3 Study Area - Example



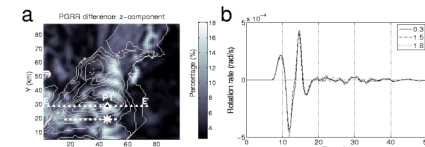
The Newport Inglewood (NI) fault system located in the Los Angeles basin is selected as study area 96x87x25.5 km (green rectangle) in the two horizontal and vertical directions, and rotated in order to have one horizontal grid axis parallel to the NI fault. The velocity model is based on the elastic part of the SCEC 3D velocity model for the Los Angeles (LA) basin (Version 3, Kohler *et al.*, 2003).

Following Guatteri *et al.*, (2004), a set of quasi-dynamic rupture processes (final slip distribution shown in the inset figure) are designed with varying hypocenter locations (red asterisks) and simulated by synthesizing the NGFs.

4 Verification - Accuracy

An M7 finite fault earthquake scenario is simulated with two subfault sizes (1.5 and 1.8 km), and the results are compared to the „continuous“ solution (0.3 km of side-length). The aim is to check if the sub-fault size of side-length 1.5 km leads to accurate results.

a. Peak ground rotation rate difference (z-component) between the solution of 1.8 km and the „continuous“ solution. Fault trace: dashed thick line. Epicenter: big white asterisk; S-wave iso-surface depth: curved thin white line. **b.** Rotation rate seismograms from different solutions (0.3, 1.5 and 1.8 km) at receiver P1 (site with worst misfit in PGRR of 18%) (a). **c.** Rotation rate seismogram profile along EE' (a) in which the depth of the basin (iso-surface of S-wave velocity of 2.0 km/s) is shown at the bottom (gray scale).



5 Rotation rate variations due to hypocenter location

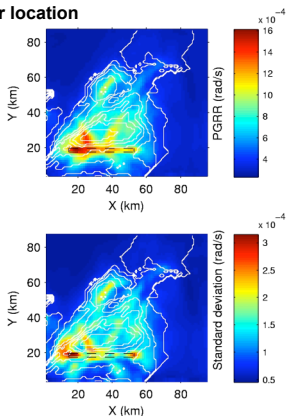
The figures show peak values and variations of 24 M7 simulations with different hypocenters, but the same slip distribution (see part 3)

Top. Maximum value of the peak ground rotation rate (PGRR) from all simulations.

Bottom. Standard deviation from the 24 simulations.

Fault trace as black dashed rectangle. S-wave iso-surface (at value of 2.0 km) depth is depicted by the curved white thin lines.

Conclusion: High value observed on the fault trace; Variations due to both directivity and basin structure.

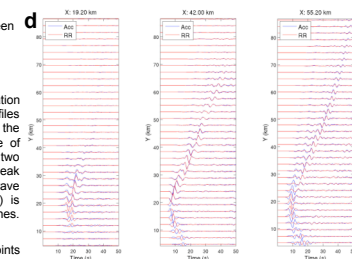


References

Guatteri, M., *et al.*, A pseudo-dynamic approximation to dynamic rupture models for strong ground motion prediction, *BSSA*, 94, pp. 2051-2063, 2004.
 Igel, H., *et al.*, Rotational motions induced by the M8.1 Tokachi-oki earthquake, September 25, 2003, *GRRL*, 32, 2005.
 Kohler, M., *et al.*, Mantle heterogeneities and the SCEC three-dimensional seismic velocity model version 3, *BSSA*, 93, pp. 753-774, 2003.
 Wang, H., *et al.*, Variations of peak ground motions due to slip histories: application to the Newport Inglewood fault, Los Angeles basin, *ESG* 2006, Third Intl. Symposium on the Effects of Surface Geology on Seismic Motion, in press, 2006.

6 Horizontal acceleration and vertical rotation rate

Comparison between translation and rotation



d. Acceleration (x-component) and rotation rate (z-component) seismogram profiles (parallel to y-axis, x-location marked at the top). **e.** Ratio between the mean value of peak acceleration amplitudes of the two horizontal components and the peak amplitude of the vertical rotation rate. S-wave iso-surface depth (at value of 2.0 km) is depicted with the curved white thin lines. Fault trace is marked as white line.

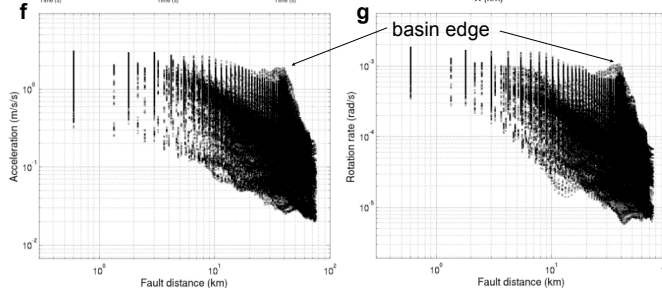
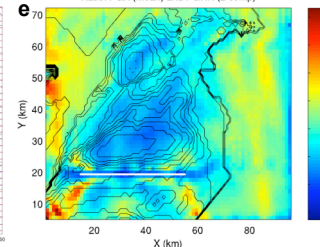
f,g. Peak amplitudes at all surface points against the fault distance for the 24 simulations (varying hypocenter).

f. Acceleration (modulus horizontal component). **g.** Rotation rate (vertical component).

Conclusions:

1. Fault parallel horizontal acceleration and rotation rate are very similar in most of the region.
2. The ratio between the peak acceleration and the rotation rate seems to correlate with the basin (in most places).
3. The peak acceleration decays in a similar way than peak rotation rate, except in the near-fault region. In the near-fault region variations of rotations seem to be smaller.

Ratio: PGA (mean) and PGRR (z-comp)



7 Conclusions

We synthesized a series of M7 earthquake scenarios with various hypocenter locations for the rotational part of seismic motion. The composite effects due to both the source and the velocity structure are discussed and compared to translations. Our conclusions are:

1. In the frequency range considered and at some distance from the fault rotation rate behaves in a similar way than transverse accelerations.
2. As observed for global wave fields, the ratio between transverse acceleration and rotation rate contains information on the local velocity structure. The synthetic data allows a rough distinction between basin and host rock area.
3. Near the source strong gradients of rotational motions are observed that may have to be taken into account for long structures (e.g., bridges) when evaluating ground motion effects.